Bull. Inst. Chem. Res., Kyoto Univ., Vol. 52, No. 1

Elastic and Inelastic Scattering of 34.4-MeV Alpha Particles by ^{90}Zr, ^{91}Zr, and ^{92}Zr.

Isao KUMABE, Masaru MATOBA*, Hiroshi OGATA, Makoto INOUE, Yasuhiko ŌKUMA**, and Tong-Hyuk KIM***

Received December 22, 1973

The angular distributions of alpha particles elastically and inelastically scattered by ^{90}Zr, ^{91}Zr, and ^{92}Zr have been measured at 34.4 MeV. Scattered alpha particles were detected with a broad-range magnetic analyser and/or a semiconductor detector. The overall energy resolution of about 70 KeV in this experiment enabled to resolve many states. The angular distributions were fitted with the predictions of the collective model using DWBA analysis. The extracted deformation parameter β_l and deformation length $\beta_l R_0$ were compared with those obtained by other workers.

I. INTRODUCTION

The inelastic scattering of alpha particles by nuclei is known to excite preferentially states of collective character. The study of the inelastic alpha scattering has proved to be a powerful tool for investigating the collective states.

The low-lying states of ^{90}Zr and of neighboring nuclei are well explained in terms of the shell model.[1~4] Therefore, it is interesting to determine how well the collective model and shell model predict inelastic scattering of alpha particles from zirconium isotopes and to see if either model gives a more consistent picture. The present study of inelastic alpha scattering by zirconium isotopes at 34.4 MeV has been intended to develop on these points of view.

Since the present experiment was begun, the results of many other experimental studies[5~17] on zirconium isotopes have become available. The studies of the inelastic alpha scattering on zirconium isotopes have been carried out at incident energies of 31 MeV[5] and above 40 MeV,[6~8] and there are no data in the incident region of 35 MeV.

In odd-mass nuclei, the quadrupole and octupole excitations would appear as multiplets due to the weak-coupling of the odd nucleon with the even-even core vibration. This splitting has actually been observed[18] in the medium weight odd-mass nuclei such as ^{59}Co, ^{63}Cu, and ^{65}Cu and has partially been explained in terms of the weak-coupling core excitation model.[19]

For the three low-lying states of ^{90}Zr, preliminary results[20] of the present experiment have been reported. In this paper more detailed results for ^{90}Zr and the results for ^{91}Zr and ^{92}Zr are described.

* 隈部 功, 的場 優: Department of Nuclear Engineering, Faculty of Engineering, Kyushu University, Fukuoka.
** 小方 寛, 井上 信, 大隈靖彦: Research Center for Nuclear Physics, Osaka University, Suita.
*** 金東赫: Institute for Physical and Mathematical Research, Pyong Sung City, D. P. R. K.

II. EXPERIMENTAL PROCEDURE

Experimental procedures were similar to those of previous investigations,[21,22] so that they are described briefly.

The 34.4-MeV alpha-particle beam from the 160-cm variable energy cyclotron at the Institute for Nuclear Study, University of Tokyo, was analysed by a beam analysing magnet and brought into a scattering chamber. The energy calibration of the beam analysing system was made with a Po-alpha source and a proton resonance device.

All targets were self-supporting metallic foils obtained from ORNL. The targets consisted of isotopically enriched ^{90}Zr (97.80%), ^{91}Zr (90.88%), and ^{92}Zr (93.22%) whose thicknesses were 1.04, 0.95, and 0.87 mg/cm^2, respectively.

Scattered alpha particles were detected by a broad-range magnetic analyser and/or an RCA Victor type C *p–n* junction detector on a turntable. Along the focal plane of the broad-range magnet, an array of 160 semiconductor detectors was set and the momentum spectra were recorded on a TMC 1024-channel pulse-height analyser. The details of this detection system[23,24] were reported elsewhere.

The pulse from the *p–n* junction detector on the turntable was amplified with a low-noise charge-sensitive preamplifier and fed into a Nuclear Data 1024-channel pulse-height analyser. A defining slit 1 mm wide and 4 mm high was placed in front of the detector and was situated 99.75 mm from the target.

For ^{90}Zr the alpha particles scattered at small angles from 15° to 40° were detected by the broad-range magnet system, while those scattered at larger angles from 40° to 60° were detected simultaneously by the *p–n* junction detector on the turntable.

For ^{91}Zr and ^{92}Zr the alpha particles scattered at a few small angles were detected by the magnet system, while those scattered at the other angles were detected by the *p–n* junction detector.

The beam current was measured by a Faraday cup and a beam integrator, and it was furthermore monitored by an NaI(Tl) scintillation counter located at an angle of 30° with the beam direction.

The energies of scattered particles were calibrated using the positions of the elastic peak and inelastic peaks corresponding to the first 2^+ state and the prominent 3^- state, whose energies were well known.[25,26]

III. EXPERIMENTAL RESULTS

Typical momentum spectra of the alpha particles scattered by ^{90}Zr, ^{91}Zr, and ^{92}Zr measured by the magnet system are shown in Figs. 1, 2, and 3, respectively. As is seen in these figures, many alpha-particle groups are well separated. The full width at half maximum was about 70 keV and 120 keV for the broad-range magnetic analyser and the *p–n* junction detector, respectively.

The angular distributions for elastic scattering are shown in Fig. 4. The angular distributions for inelastic scattering are shown in Figs. 5 ~ 10.

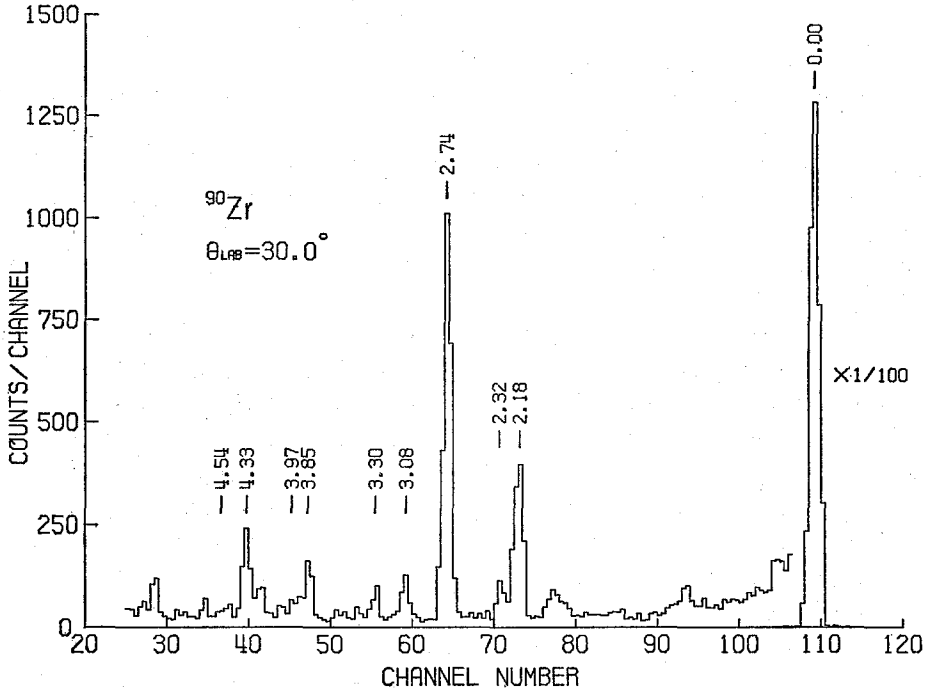

Fig. 1. Typical momentum spectrum of alpha particles scattered by ^{90}Zr at a laboratory angle of 30°. The energy levels corresponding to the peaks are shown in the upper part of the figure.

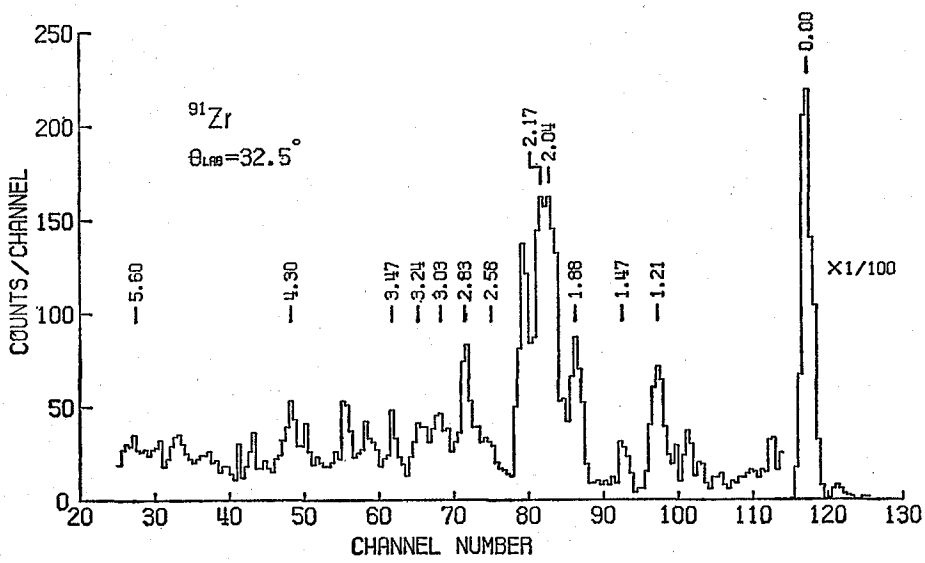

Fig. 2. Typical momentum spectrum of alpha particles scattered by ^{91}Zr at a laboratory angle of 32.5°. The energy levels corresponding to the peaks are shown in the upper part of the figure.

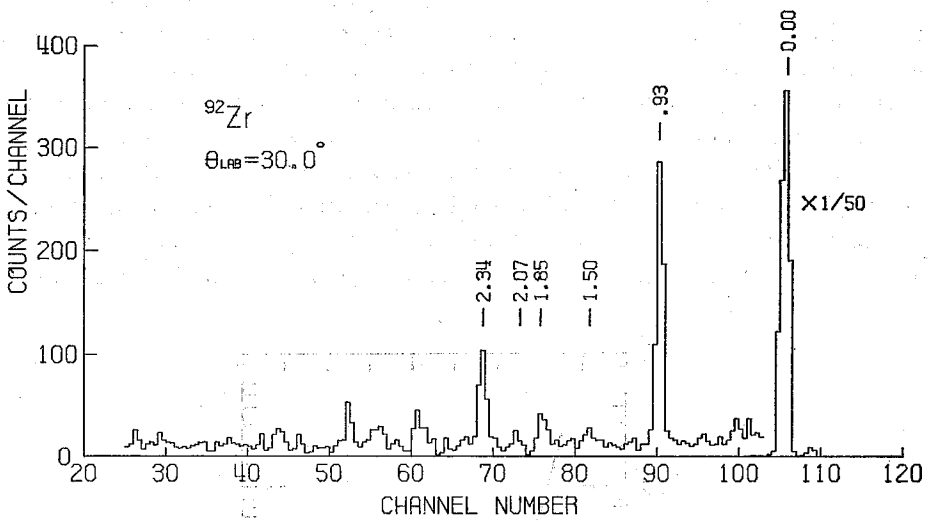

Fig. 3. Typical momentum spectrum of alpha particles scattered by ^{92}Zr at a laboratory angle of 30°. The energy levels corresponding to the peaks are shown in the upper part of the figure.

IV. DATA ANALYSIS

As described in the introduction, our primary intention was to determine how well the collective model and shell model predict inelastic scattering of alpha particles from zirconium isotopes and to see if either model gives a more consistent picture. For the interpretation of single-particle shell model, however, detailed analyses for zirconium isotopes have already been published by many authors for inelastic proton scattering[9,10,13] and by Bingham *et al.*[8] for inelastic alpha scattering. Even though the incident energy and/or the projectile are different, most conclusions of their analysis are expected to be consistent with our experimental results. Therefore, in the present paper the DWBA calculation is limited to the collective one-phonon excitation.

IV–1 The Optical Model

For the elastic angular distributions, an optical-model analysis was performed. The experimental angular distribution does not cover a wide angular range, so there will be no need to use the most general optical potential in which the real and imaginary parts have independent parameters. We used, therefore, the four parameter potential and the Coulomb potential from a uniformly charged sphere of radius $r_c A^{1/3}$.

The assumed optical potential is written as

$$U(r)=V_c(r)-(V+iW)(e^x+1)^{-1},$$

$$x=(r-r_0A^{1/3})/a,$$

where $V_c(r)$ is the Coulomb electrostatic potential, V and W are the depths of the real and imaginary parts, respectively, of the nuclear optical potential, and $r_0A^{1/3}$ and a are the interaction radius and the diffuseness parameter, respectively.

Fits to the data were obtained by varying the parameters of the potential so as to minimize the mean square deviation between the experimental and predicted cross sections. The minimization was performed using an automatic search routine.[27]

The quantity χ^2/point was calculated assuming relative cross-section errors of 5%. As is well known,[28] alpha-particle scattering does not yield a unique optical potential. In Table I, two sets of potential parameters of depth V of about 50 and 200 MeV are given for each isotope. The angular distributions predicted by the potentials 2, 4, and 6 are compared with the experimental angular distributions in Fig. 4. The potentials 1, 3, and 5 reproduced nearly the same angular distributions as those predic-

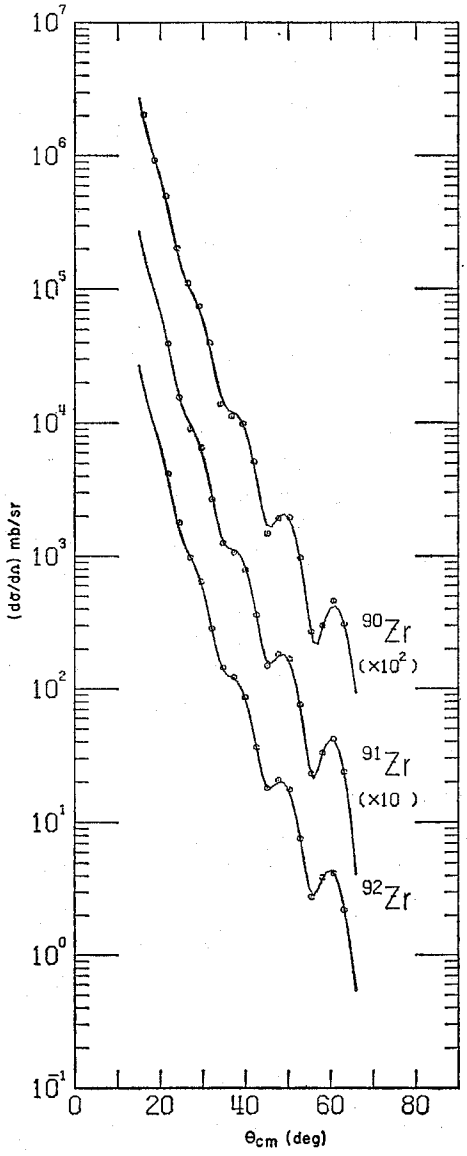

Fig. 4. Measured elastic scattering from ^{90}Zr, ^{91}Zr, and ^{92}Zr, and the optical model fits using the potential 2, 4, and 6, respectively, of Table I.

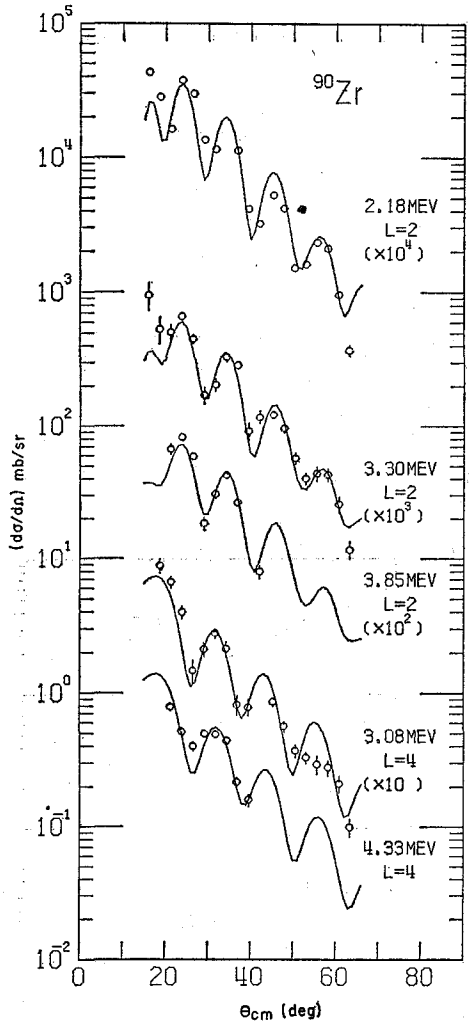

Fig. 5. Measured angular distributions for inelastic scattering leading to the various states of ^{90}Zr. The solid curves are the DWBA predictions.

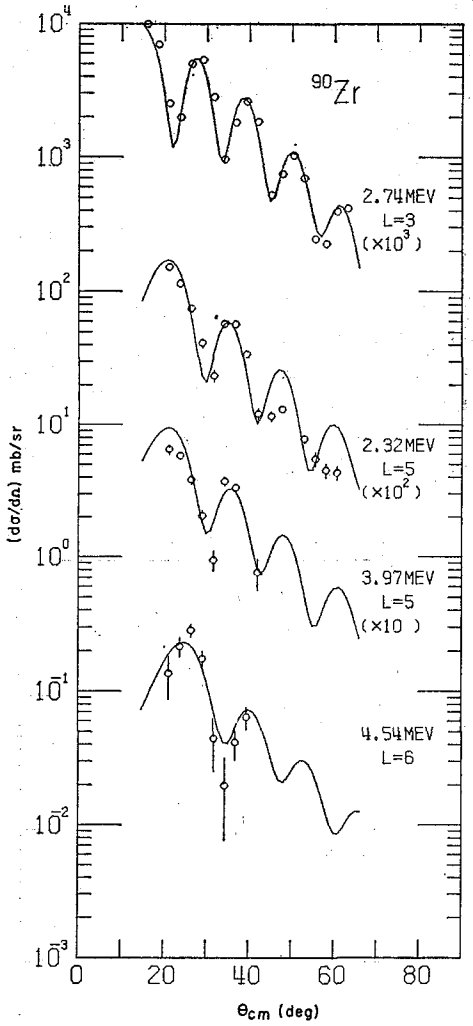

Fig. 6. Measured angular distributions for inelastic scattering leading to the various states of ^{90}Zr. The solid curves are the DWBA predictions.

Table I. Optical Potentials for 34.4 MeV Alpha Particles on ^{90}Zr, ^{91}Zr, and ^{92}Zr.

		V (MeV)	W (MeV)	r_0 (fm)	a (fm)	r_c (fm)	χ^2/n
^{90}Zr	1	45.857	11.246	1.5627	0.5775	1.30	1.32
	2	194.482	23.249	1.3750	0.5707	1.30	1.83
^{91}Zr	3	56.073	14.583	1.5027	0.6112	1.30	1.06
	4	213.920	27.847	1.3409	0.5939	1.30	0.68
^{92}Zr	5	54.946	15.602	1.5167	0.5935	1.30	1.08
	6	212.077	33.182	1.3595	0.5765	1.30	0.89

ted by the potentials 2, 4, and 6, respectively.

The potentials 2, 4, and 6 were used for the following DWBA calculation.

IV-2 DWBA Analysis

The first order collective excitation was assumed in the calculation.

The form factor of the interaction potential is

$$f(r)=\frac{R_0 V}{a}\frac{dU(r)}{dr},$$

where $U(r)$ is the optical potential used for calculation in the elastic scattering and R_0 is the nuclear radius. The deformation parameters β_l's were determined by normalizing the individual calculated cross sections to the corresponding experimental data.

For these calculations, the DWBA computer code INS-DWBA 2[29] was used. The results of the DWBA calculations are shown in Figs. 5~10. The agreement be-

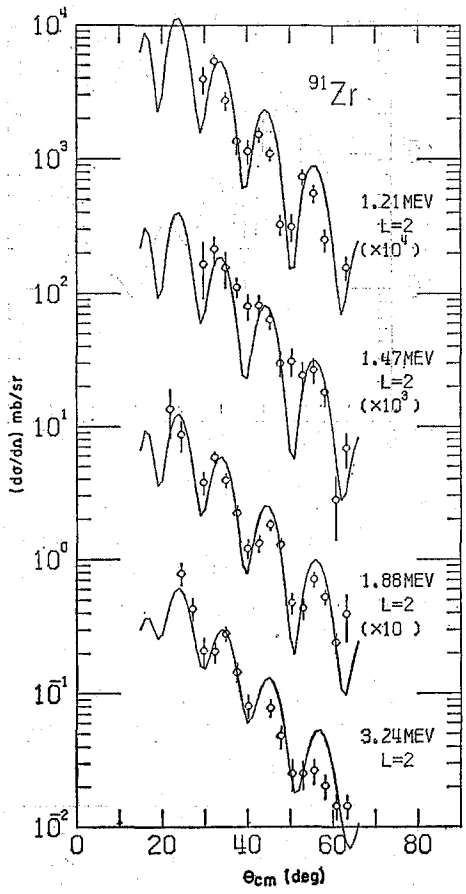

Fig. 7. Measured angular distributions for inelastic scattering leading to the various states of ^{91}Zr. The solid curves are the DWBA predictions.

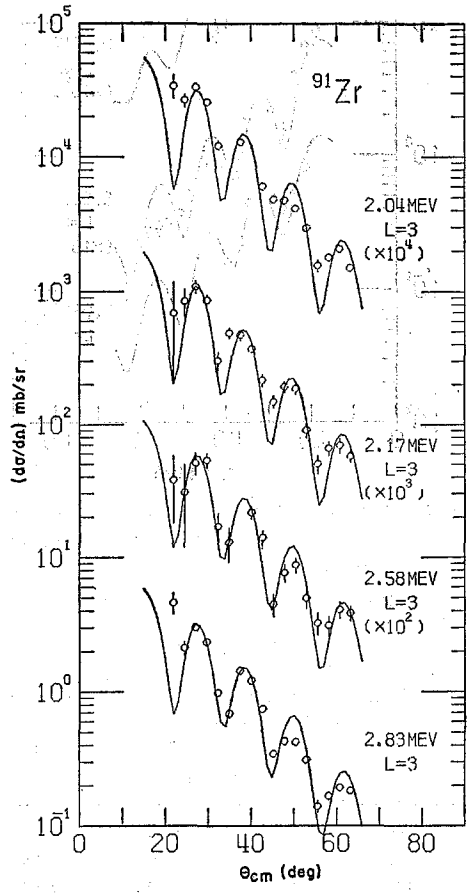

Fig. 8. Measured angular distributions for inelastic scattering leading to the various states of ^{91}Zr. The solid curves are the DWBA predictions.

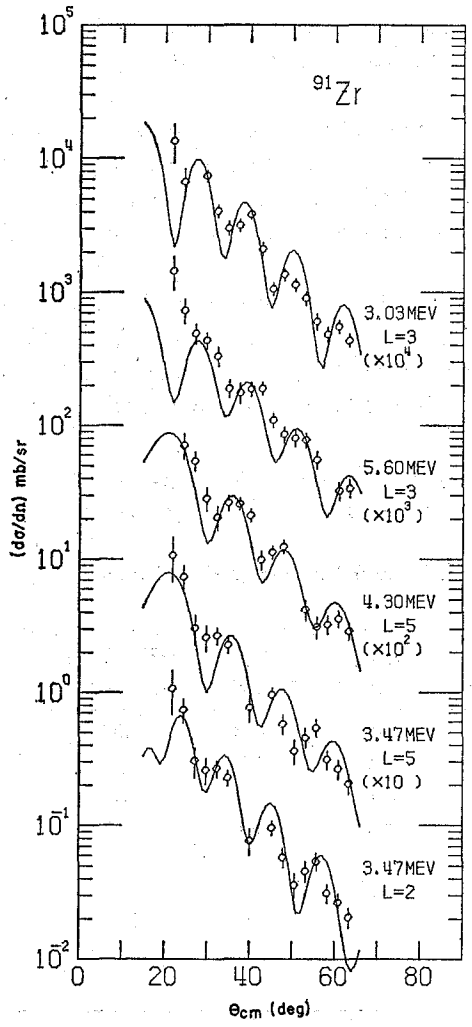

Fig. 9. Measured angular distributions for inelastic scattering leading to the various states of ^{91}Zr. The solid curves are the DWBA predictions.

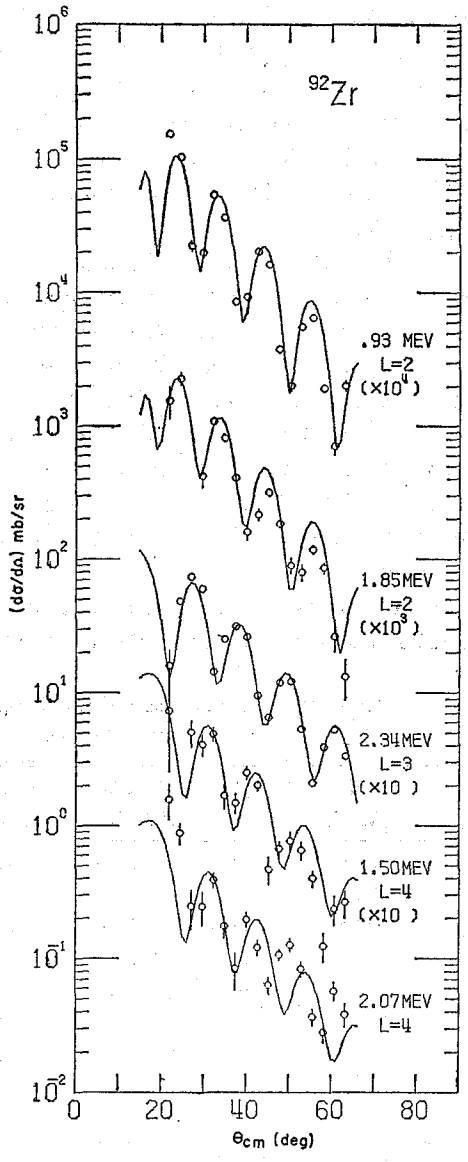

Fig. 10. Measured angular distributions for inelastic scattering leading to the various states of ^{92}Zr. The solid curves are the DWBA predictions.

tween theory and experiment is sufficiently good to enable us to make spin and parity assignments. All the curves include Coulomb excitation.

Martens and Bernstein[5] have analysed the ^{90}Zr(α, α') reaction at 31 MeV and have pointed out that the long-rang $1/r^{l+1}$ dependence of the Coulomb form factor implies the need to consider large impact parameters and correspondingly large angular momenta.

The trial calculations for $l=2$ and $l=3$ with Coulomb excitation for $L_{max}=30$,

45, and 50 were carried out. The results show that there is a large difference between $L_{max}=30$ and $L_{max}=45$ in both cases. However, there is a small difference of a few percent between $L_{max}=45$ and $L_{max}=50$ beyond 20° for $l=2$, while there is no appreciable difference between $L_{max}=45$ and $L_{max}=50$ beyond 15° for $l=3$. Therefore, we concluded that the convergence was approximately obtained for $L_{max}=50$. Thus all the DWBA calculations shown in Figs. 5~10 were carried out for $L_{max}=50$ and $R_{max}=25$ fm.

Trial calculations for a complex form factor including Coulomb excitation effect were also made. Calculated differential cross sections are a few percent larger than those for the real form factor but the patterns of calculated curves are very similar to those for the real form factor, so that this additional complication was not included in the remainder of the calculations.

As is well known, the deformation parameter β_l for a given state differs considerably for different optical model parameters, but the deformation length $\beta_l R_0$ differs by only a few percent. It is reasonable to compare the $\beta_l R_0$ values rather than the β_l values for the experimental data obtained at different bombarding energies and with different projectiles.

The values of the deformation length $\beta_l R_0$ for ^{90}Zr and ^{92}Zr together with the results obtained by other workers are presented in Table II and III, respectively.

Table II. Values of the Deformation Length $\beta_l R_0$ (in fm) in ^{90}Zr Derived from the Present Data and Other Results.

E (MeV)	J^π	(α, α') 34 MeV	(α, α') 31 MeV[a]	(α, α') 65 MeV[b]	(p, p') 18 MeV[c]	$(^3\mathrm{He}, ^3\mathrm{He}')$ 44 MeV[d]
2.18	2^+	0.47	0.50	0.40	0.38	0.52
3.30	2^+	0.22	0.20	0.25		
3.85	2^+	0.26	0.26	0.30		0.33
2.74	3^-	0.83	0.89	0.84	0.88	0.78
3.08	4^+	0.24	0.23		0.22	
4.33	4^+	0.35	0.31	0.33		
2.32	5^-	0.39	0.38		0.41	
3.97	5^-	0.31	0.23			
4.54	6^+	0.18				

a) ref. 5. b) ref. 8. c) ref. 9. d) ref. 16.

Table III. Values of the Deformation Length $\beta_l R_0$ (in fm) in ^{92}Zr Derived from the Present Data and Other Results.

E (MeV)	J^π	(α, α') 34 MeV	(α, α') 65 MeV[a]	(p, p') 19 MeV[b]	(d, d') 15 MeV[c]
0.93	2^+	0.75	0.74	0.74	0.63
1.85	2^+	0.37	0.34	0.31	
2.34	3^-	0.92	1.06	1.02	0.88
1.50	4^+	0.32	0.38	0.38	
2.07		0.29 (4^+)		0.24 (3^-)	

a) ref. 8. b) ref. 10. c) ref. 15.

V. DISCUSSION

V–1 Elastic Scattering

For alpha scattering, it is well known[28] that there are several sets of optical model parameters which give almost equally satisfactory fits to the experimental data.

A native picture of the alpha-nucleus interaction could envisage it as a simple superposition of four nucleon-nucleus optical potentials, suitable averaged over the internal motion of the alpha particle. Such a potential would have a real depth of order 200 MeV. As seen in Table I, the present case shows a preference for the sets of potential parameters of depth V of about 200 MeV.

V–2 Inelastic Scattering for ^{90}Zr

As is seen in Figs. 5 and 6, the phases of the measured angular distributions are in fairly good agreement with the DWBA calculations, but the cross sections for a few states fall off with angle more rapidly than the calculated ones. Especially, the measured angular distribution for the 2.74-MeV (3^-) state is in good agreement with the calculated one. It deserves some notice that the measured angular distribution for the 4.54-MeV (6^+) state is in good agreement with the calculated one.

Inelastic scattering experiments for ^{90}Zr were carried out at different bombarding energies and with different projectiles by many workers. As seen in Table II, $\beta_l R_0$ values obtained by many workers[5,8,9,16] are in fairly good agreement with each other. However, the agreement of $\beta_l R_0$ values for the 2.18-MeV (2^+) state is not so good, as those for 2.74-MeV (3^-) state is very good. This fact may indicate that the collective model is a poorer description of the 2.18-MeV excitation than of the 2.74-MeV excitation.

V–3 Inelastic Scattering for ^{92}Zr

As is seen in Fig. 10, the experimental angular distributions for the 0.93-, 1.85-, and 2.34-MeV states are in good agreement with the DWBA predictions, while those for the 1.50- and 2.07-MeV states are not so good.

Jolly[15] found that for 15-MeV deuterons the 1.85-MeV(2^+) and 1.50-MeV(4^+) states have similar angular distributions, and he concluded that they, together with the 1.38-MeV (0^+) state, might be members of a two-phonon triplet. To analyse two-phonon states, coupled-channel calculations[30] are ordinarily used.

For the two-phonon states of ^{60}Ni, our previous results[31] have been analysed by Tamura[32] with the coupled-channel method and have been successfully explained as an interference effect between two possible modes for exciting the two-phonon states, *i.e.*, a direct transition and a multiple transition.

The angular distribution for the 1.50-MeV state shows some indication of slipping out of phase with the single-excitation prediction at larger angles. This tendency is similar to that in the case of ^{60}Ni. This situation indicates that the 1.50-MeV state may be the two-phonon state, but that there is a serious objection[33,34] to the traditional phonon model at least at the present incident energy. The same conclusions have been reached also with shell-model calculations.[35]

Jolly[15] suggested that the 2.07-MeV group seems to be a mixture of $l=2$ and $l=3$ or 4 transitions, while Stautberg *et al.*[10] analysed their (p, p') data as $l=3$ for the 2.07-MeV group. The present result seems to support Jolly's suggestion.

$\beta_l R_0$ values obtained in the present experiment are in fairly good agreement with those obtained by other workers[8,10,15] as seen in Table III.

V-4 Inelastic Scattering for ^{91}Zr

The measured angular distributions shown in Fig. 2 are for groups of unresolved states except for a few low lying states, so that precise spectroscopic information is not expected to be obtained.

The angular distributions for the 1.21-, 1.47-, and 1.88-MeV groups fit to the calculated curves for $l=2$. If these groups arise primarily from weak-coupling of a $d_{5/2}$ neutron to the ^{90}Zr core excited to the 2^+ state at 2.18 MeV, the sum of the cross sections for these groups should be the same as the cross section for the excitation of the 2.18-MeV (2^+) state of ^{90}Zr. Experimentally the sum is about 0.7 times.

The angular distributions for the 2.04-, 2.17-, 2.58-, 2.83-, and 3.03-MeV groups fit to the calculated curves for $l=3$. If these groups arise primarily from weak-coupling

Table IV. Excited States in ^{91}Zr

Present work				14 MeV (p, p')[a]			19 MeV (p, p')[b]	
E_x (MeV)	l	J^π	β_l	E_x (MeV)	l	β_l	E_x (MeV)	l
1.21	2	$1/2^+$	0.16	1.19	2	0.17	1.205	2
1.47	2	$5/2^+$	0.05	1.45	2	0.09	1.475	2
1.88	2	$7/2^+$	0.08	1.86	2	0.11	1.880	2
2.04	3	$(3/2, 5/2, 7/2^-)$		2.02	3		2.040	(2)
2.17	3	$(11/2^-)$	(0.11)	2.15	3	(0.24)	2.160	3
							2.200	
				2.32			2.320	
				2.35			2.385	
2.58	3	$(1/2^-)$	(0.21)	2.54	3	(0.24)	2.565	(2)
							2.630	3
		$(3/2, 5/2, 7/2^-)$		2.67	3		2.690	3
							2.755	3
2.83	3	$(9/2^-)$	(0.22)	2.79	3	(0.20)	2.815	3
							2.910	
3.03	3	$(3/2, 5/2, 7/2^-)$		3.01	3		3.030	3
				3.08	2		3.100	
3.24				3.26			3.225	
							3.300	
3.47				3.45	(5)		3.475	
4.3	(5)							
5.6	(3)							

a) ref. 14. b) ref. 13.

of a $d_{5/2}$ neutron to the ^{90}Zr core excited to the 3^- state at 2.74 MeV, the sum of the cross sections for these groups should be the same as the cross section for the excitation of the 2.74-MeV (3^-) state of ^{90}Zr. The sum is about 1.6 times.

The weak-coupling core excitation model[19] predicts that the cross section for each member of the multiplet will be proportional to $2J+1$, where J is a spin of the final state. The deduced β_2 and β_3 values are listed in Table IV. The β_2 value ranges from 0.05 to 0.16 and the β_3 value ranges from 0.11 to 0.22. This fact and the fact concerning with the summed cross sections show that this model may not be a good description in this nucleus.

For the 2.04-MeV group the angular distribution obtained from the 14-MeV (p, p') work[14] fits to the calculated curve for $l=3$, while that obtained by the 19-MeV (p, p') work[13] fits to the calculated curve for $l=2$. The present data support $l=3$. On the other hand, the spin-parity of the 2.04-MeV state has already been assigned[26] to be $3/2^+$ which corresponds to $l=2$. This discrepancy cannot be explained in this stage.

For the 3.47-MeV group Awaya *et al.*[14] suggested $l=5$ transition. As seen in Fig. 9, the angular distribution obtained by us fits to the calculated curve for $l=2$ rather than $l=5$.

The angular distributions for the 4.3- and 5.6-MeV groups fit to the calculated curves for $l=5$ and $l=3$, respectively.

ACKNOWLEDGMENTS

The authors would like to dedicate this paper to the memory of the late Professor Y. Uemura, who encouraged us for the study of inelastic alpha scatterings.

The authors wish to thank Professor T. Yanabu for interests and encouragements throughout this work and to Mr. T. Nomaguchi for the assistance in taking the experimental data. They are also grateful to the cyclotron crew of INS for their kind operation of the cyclotron.

REFERENCES

(1) K. W. Ford, *Phys. Rev.*, **98**, 1516 (1955).
(2) B. F. Bayman, A. S. Reiner, and R. K. Sheline, *Phys. Rev.*, **115**, 1627 (1959).
(3) S. Cohen, R. D. Lawson, M. H. Macfarlane, and M. Soga, *Phys. Lett.*, **10**, 195 (1964).
(4) N. Auerbach and I. Talmi, *Nucl. Phys.*, **64**, 458 (1965).
(5) E. J. Martens and A. M. Bernstein, *Nucl. Phys.*, **A117**, 241 (1968).
(6) D. L. Hendrie and G. W. Farwell, *Phys. Lett.*, **9**, 321 (1964).
(7) H. W. Broek and J. L. Yntema, *Phys. Rev.*, **138**, B334 (1965).
(8) C. R. Bingham, M. L. Halbert, and R. H. Bassel, *Phys. Rev.*, **148**, 1174 (1966).
(9) W. S. Gray, R. A. Kenefick, J. J. Kraushaar, and G. R. Satchler, *Phys. Rev.*, **142**, 735 (1966).
(10) M. M. Stautberg and J. J. Kraushaar, *Phys. Rev.*, **151**, 969 (1966).
(11) J. L. Dubard and R. K. Sheline, *Bull. Amer. Phys. Soc.*, **12**, 1035 (1967).
(12) K. Matsuda, H. Nakamura, I. Nonaka, H. Taketani, T. Wada, Y. Awaya, and M. Koike, *J. Phys. Soc. Japan*, **22**, 1311 (1967).
(13) H. P. Block, G. D. Thijs, J. J. Kraushaar, and M. M. Stautberg, *Nucl. Phys.*, **A127**, 188 (1969).

(14) Y. Awaya, K. Matsuda, N. Nakanishi, S. Takeda, and T. Wada, *J. Phys. Soc. Japan,* **27**, 1087 (1969).
(15) R. K. Jolly, *Phys. Rev.,* **139**, B318 (1965).
(16) E. F. Gibson, J. J. Kraushaar, B. W. Ridley, M. E. Rickey, and R. H. Bassel, *Phys. Rev.,* **155**, 1208 (1967).
(17) D. E. Rundquvist, M. K. Brussel, and A. I. Yavin, *Phys. Rev.,* **168**, 1287 (1968).
(18) See, for instance, A. L. McCarthy, and G. M. Crawleys, *Phys. Rev.,* **150**, 935 (1966).
(19) A. de-Shalit, *Phys. Rev.,* **122**, 1530 (1961).
(20) H. Ogata, S. Tomita, M. Inoue, Y. Ōkuma, and I. Kumabe, *Phys. Lett.,* **17**, 280 (1965).
(21) I. Kumabe, H. Ogata, T. H. Kim, M. Inoue, Y. Ōkuma, and M. Matoba, *J. Phys. Soc. Japan,* **25**, 14 (1968).
(22) M. Inoue, *Nucl. Phys.,* **A119**, 449 (1968).
(23) T. Kobayashi and S. Takayanagi, *Nucl. Instr. and Meth.,* **53**, 77 (1967).
(24) K. Matsuda, I. Nonaka, K. Omata, K. Yagi, and M. Koike, *Nucl. Instr. and Meth.,* **53**, 82 (1967).
(25) J. B. Ball and R. L. Auble, *Phys. Rev.,* **C**, **4**, 196 (1971).
(26) Nuclear Data Sheets, **8**, No. 6 (1972).
(27) M. Igarashi, "Automatic Search for Optical Potential Parameters" INS-PT-26 (1970).
(28) Lynne McFadden and G. R. Satchler, *Nucl. Phys.,* **84**, 177 (1966).
(29) M. Kawai, K. Kubo, and H. Yamaura, "INS-DWBA 2" INS-PT-9 (1965).
(30) T. Tamura, *Rev. Mod. Phys.,* **37**, 679 (1965).
(31) I. Kumabe, H. Ogata, S. Tomita, M. Inoue, and Y. Ōkuma, *Phys. Lett.,* **17**, 45 (1965).
(32) T. Tamura, *Progr. Theor. Phys.* Suppl., **37** & **38**, 383 (1966).
(33) A. Tokunaga, *Progr. Theor. Phys.,* **37**, 315 (1967).
(34) M. Yamamura, A. Tokunaga, and T. Marumori, *Progr. Theor. Phys.,* **37**, 336 (1967).
(35) L. S. Hsu and J. B. French, *Phys. Lett.,* **19**, 135 (1965);
S. Cohen, R. D. Lawson, M. H. MacFarlane, S. P. Pandya, and M. Soga, *Phys. Rev.,* **160**, 903 (1967);
Y. K. Gambhir and R. Raj. *Phys. Rev.,* **161**, 1125 (1967);
N. Auerbach, *Phys. Rev.,* **163**, 1203 (1967).